Received 4 April 2024; revised 28 April 2024; accepted 7 May 2024. Date of publication 10 May 2024; date of current version 18 April 2025.

Digital Object Identifier 10.1109/OJCOMS.2024.3399728

Multi-Stream Transmission for Directional Modulation Network via Distributed Multi-UAV-Aided Multi-Active-IRS

KE YANG[1], RONGEN DONG[1], WEI GAO[1], FENG SHU[1,2] (Member, IEEE), WEIPING SHI[3], YAN WANG[1], XUEHUI WANG[1], AND JIANGZHOU WANG[4] (Fellow, IEEE)

(Special Issue on Emerging Modulation Techniques Towards 6G Networks)

[1]School of Information and Communication Engineering, Hainan University, Haikou 570228, China
[2]School of Electronic and Optical Engineering, Nanjing University of Science and Technology, Nanjing 210094, China
[3]School of Network and Communication, Nanjing Vocational College of Information Technology, Nanjing 210023, China
[4]School of Engineering, University of Kent, CT2 7NT Canterbury, U.K.

CORRESPONDING AUTHORS: F. SHU, R. DONG, AND W. GAO (e-mail: shufeng0101@163.com; dre2000@163.com; gaowei@hainanu.edu.cn)

This work was supported in part by the National Natural Science Foundation of China under Grant U22A2002 and Grant 62071234; in part by the Hainan Province Science and Technology Special Fund under Grant ZDKJ2021022; in part by the Scientific Research Fund Project of Hainan University under Grant KYQD(ZR)-21008; in part by the Collaborative Innovation Center of Information Technology, Hainan University under Grant XTCX2022XXC07; and in part by the National Key Research and Development Program of China under Grant 2023YFF0612900.

ABSTRACT Active intelligent reflecting surface (IRS) is a revolutionary technique for the future 6th generation mobile networks. The conventional far-field single-IRS-aided directional modulation (DM) networks have only one (no direct path) or two (existing direct path) degrees of freedom (DoFs). This means that there are only one or two streams transmitted simultaneously from base station to user and will seriously limit its rate gain achieved by IRS. How to create multiple DoFs more than two for DM? In this paper, single large-scale IRS is divided to multiple small IRSs and a novel multi-IRS-aided multi-stream DM network is proposed to achieve a point-to-point multi-stream transmission by creating K (≥ 3) DoFs, where multiple small IRSs are placed distributively via multiple unmanned aerial vehicles (UAVs). The null-space projection, zero-forcing (ZF) and phase alignment are adopted to obtain the transmit beamforming, receive beamforming and phase shift matrix (PSM), respectively, called NSP-ZF-PA. Here, K PSMs and their corresponding beamforming vectors are independently optimized. The weighted minimum mean-square error (WMMSE) algorithm is involved in alternating iteration for the optimization variables by introducing the power constraint on IRS, named WMMSE-PC, where the majorization-minimization (MM) algorithm is utilized to address the total PSM. To achieve a lower computational complexity, a maximum trace method, called Max-TR-SVD, is proposed by optimizing the PSM of all IRSs. Simulation results have shown that the proposed NSP-ZF-PA performs much better than Max-TR-SVD in terms of rate. In particular, the rate of NSP-ZF-PA with sixteen small IRSs is about five times that of NSP-ZF-PA with combining all small IRSs as a single large IRS. Thus, a dramatic rate enhancement may be achieved by multiple distributed IRSs.

INDEX TERMS Active multi-IRS, DM, DoF, beamforming.

I. INTRODUCTION

NOWADAYS, the rapid development of wireless network has greatly improved one's lives. Due to its ultra-high rate and direction of arrival (DOA) measurement precision, the large-scale multi-input multi-output (MIMO) array has already become a research hotspot in academic and industry field [1], [2], [3]. The deep-learning (DL) transmission design and receiver scheme for physical layer communication network were investigated in [4]. With the upgrade of meta-materials, passive intelligent reflecting

surface (IRS) is getting more and more attention from researchers for its possible and potential applications in future wireless networks [5]. For the problems of MIMO channel estimation and signal detection in the model-driven DL network, [6] developed an orthogonal approximate message passing (OAMP) detection algorithm to solve it, and validated that the proposed OAMP algorithm performed better than traditional detectors. Passive large IRS is an important physical layer technology of B5G systems, since it can enhance network's quality of service, extend coverage, and reduce power consumption [7]. Passive IRS contains a large quantity of affordable reflective elements, it is controlled intelligently, and can effectively control the wavefront of the incident signals. Passive IRS intelligently configures the wireless environment between base station (BS) and user to improve communication rate [8], [9], [10]. In [11], the authors made an investigation of the design of beamforming methods, the detection of passive IRS channel, the equipment of IRS, and advised that the machine learning technique may be an useful way to make an optimal deployment of IRS. There are many explorations in the passive IRS, which were combined with the practical application. The authors in [12] designed a prototype of passive IRS-aided wireless network and verified that this prototype could reduce the cost of hardware and power. Reference [13] introduced the passive IRS to improve the stability of millimeter wave communication, and the co-optimization was utilized to obtain the phase shift matrix (PSM) of IRS and beamforming of transmitter. The energy conservation in passive IRS-aided network has also been investigated in [14], [15], the former used the gradient descent and fractional programming to figure out the power distribution and phase shift, while the latter utilized the semidefinite relaxation (SDR) to acquire the PSM at IRS. In [16], the authors proposed a novel IRS-aided network to achieve the amplitude-phase modulation by controlling the ON-OFF state and phase shift. The authors in [17] proposed a method to estimate channel, cyclic-prefix single-carrier cyclic delay diversity with the aid of IRS to alternately transmit the pilots and data, which is robust in time-varying conditions.

Active IRS can overcome the inherent physical limitation, the effect of double fading introduced by IRS, and further increase the rate gain. It is mainly due to the fact that the active IRS reflects signals with an amplification capability while the passive IRS just adjusts the phase of incident signals and no amplitude. And active IRS can attain more throughput than passive IRS for small-scale or medium-scale scenarios [18], [19], [20], [21]. Similarly, active IRS can also be combined with other technologies. The alternating iteration is exploited to alternately optimize the beamforming at BS and IRS, and it was shown that the two active IRSs can make a higher rate gain than one or two passive IRSs in [22]. The authors in [23] researched the networks of non-orthogonal multiple access with the help of the active IRS, the achievable rate was promoted by utilizing SDR and minimum-mean-square-error (MMSE). The norm and normalized beamforming vector were alternately iterated in [24] to acquire the optimization approximation signal-to-noise ratio (SNR). The authors in [25] used the linear minimum mean square error to estimate the cascaded channel in the active IRS-aided network. Reference [26] employed average SNR at active IRS to strengthen the capability of network and revealed that the SNR at receiver is proportional to the SNR at IRS. The authors in [27] derived the security and dependability in an active IRS-aided network by analyzing the outage and intercept probability, and it was verified that active IRS performs better than passive IRS.

Directional modulation (DM) technique can enhance the pattern of antenna array to the target direction and weaken it in unexpected directions. And it is widely used in physical-layer security field, which have been investigated in [28], [29], [30]. The authors in [31] utilized the artificial noise (AN) projection and phase alignment to transmit signals securely and accurately in DM network. The IRS can also be combined with DM networks to overcome the limitation that traditional DM network can only transmit one privacy data stream. The passive IRS in [32] was used to create more than one transmit path, the null-space projection and alternating iterative algorithm were utilized to promote the secrecy rate (SR). In [33], to enhance the communication security in the DM network with passive IRS, the PSM and receive beamforming were optimized by alternating iteration, and the zero forcing (ZF) method was also been applied to reduce complexity. To raise the performance of the DM network with a passive IRS, [34] utilized AN and ZF to optimize the beamforming in DM network with an active IRS and achieved obvious SR enhancement than no IRS.

For a far-field single IRS-aided DM network, there is only one (no direct path) or two (existing direct path) degrees of freedom (DoFs). This will seriously limit its rate gain achieved by IRS. According to the basic principle of MIMO network, DoF plays a prominent role in rate improvement. In this paper, a large-scale active IRS is partitioned into K small distributed IRSs to create a large number of DoFs (≥ 3), where each UAV hangs one small IRS. This will lead to the maximum DoF of the total network being K or $K+1$. In other words, in such a DM network, a multi-stream point-to-point transmission may be achieved over single IRS-aided DM network to make a significant rate enhancement. Our main contributions in this paper can be concluded as follows:

1) To achieve a significant rate improvement, a novel multi-IRS-aided multi-stream DM network is proposed. In other words, a large-scale IRS should be splitted into several smaller IRSs and these IRSs should be distributedly placed in free space to create more DoF. This new DM network may implement a point-to-point multi-stream transmission by creating more DoFs than traditional single-IRS DM network due to a distributed multi-IRS network with each UAV hanging one IRS. When the number of small IRSs is K, the achievable maximum DoF is K or $K+1$, where K means the direct transmission link from BS to user is

blocked and $K+1$ means the direct communication link from BS to user exists. In this paper, we will focus the former in order to simplify the design of beamforming. However, the beamforming methods may be extended to the latter with some modifications.

2) To eliminate the interference among different data-streams associated with small IRSs, the null-space projection (NSP) at BS and receive zero-forcing (ZF) at user is adopted to design the beamforming of transmitter and receiver. This will lead to the fact that K streams are independently transmitted along the corresponding small IRSs. This method is called NSP-ZF, and has a closed-form and thus low-complexity. Phase alignment method is utilized to calculate the PSM of each small IRSs. We call this method as NSP-ZF-PA, where PA is short for phase alignment. And simulation results have shown that the proposed NSP-ZF-PA performs much better than proposed Max-TR-SVD in terms of rate. In particular, the rate of NSP-ZF-PA with sixteen sub-IRSs is about five times that of NSP-ZF-PA with all small IRSs combining a single large IRS.
3) In the above method, the PSMs of all IRSs are individually optimized. Now, all small IRSs are viewed as a large virtual IRS, the weighted minimum mean-square error (WMMSE) is proposed with power constraint (PC) on active IRS. Due to the determinant, the original optimization problem is rewritten as a more tractable form. The alternating iteration is utilized to acquire the beamforming at transmitter, PSM and beamforming at receiver. The majorization-minimization (MM) algorithm is involved to obtain the optimization PSM of this large-scale IRS. This method is called WMMSE-PC. To achieve a low computational complexity, the transmit and receive beamforming are designed by singular value decomposition (SVD). Then, a maximum trace method is proposed to optimize the total PSM of all sub-IRSs. Due to its quadratic form, its closed form is directly derived. This methods is called Max-TR-SVD. According to simulation result, we found that the WMMSE-PC has a better performance than NSP-ZF-PA when the power at IRS is low, while having a worse performance than NSP-ZF-PA when the power at IRS is high. And the proposed WMMSE-PC performs also better than Max-TR-SVD about rate.

The remainder is mainly organized as follows. The system model and DoF analysis are shown in Section II. Section III denotes the proposed three methods. The performance and complexity analysis are shown in IV. Simulation results we obtained are presented in V. Finally, conclusions are provided in VI.

Notations: The sign $\mathbb{C}$ presents the set of complex. Signs $[\cdot]^*$, $[\cdot]^\dagger$, $[\cdot]^T$, $[\cdot]^{-1}$ and $[\cdot]^H$ express the conjugate, pseudo-inverse, transpose, inverse and conjugate-transpose operations, respectively. The notations $\|\cdot\|$ and $\|\cdot\|_F$ stand for the 2-norm and F-norm operations, respectively. The diag$(\cdot)$ signifies the diagonal operator. The $\mathbf{I}_N$ is an $N \times N$ unit matrix. The $Tr(\cdot)$ and $|\cdot|$ denote the trace and determinant operation. The notations $Re\{s\}$ and $arg(s)$ indicate the real part and the argument of the value s. Signs $\mathbb{E}\{\cdot\}$, $\odot$ and $ln(\cdot)$ express the expectation, Hadamard product and natural logarithm operators, respectively. The sign $\mathcal{CN}(\mu, \sigma^2)$ signifies the complex Gaussian distribution with mean μ and variance σ^2.

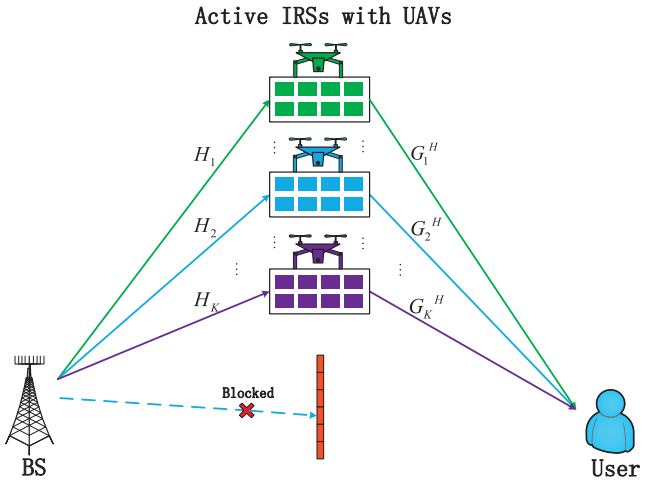

(a) Splitting a large-scale active IRS into K smaller IRSs.

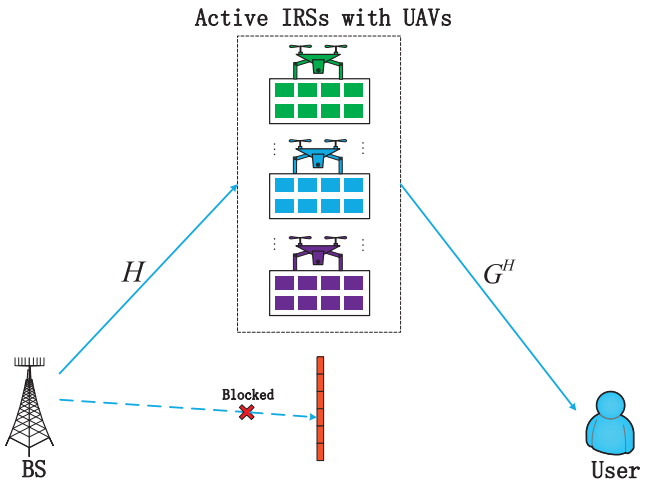

(b) Viewing K smaller IRSs as a large virtual IRS.

FIGURE 1. System model of a distributed multi-UAV-aided multi-active-IRS network.

II. SYSTEM MODEL AND DOF ANALYSIS

A. PARTITIONING A LARGE-SCALE ACTIVE IRS INTO K SMALLER IRSS

In Fig. 1(a), we plot a distributed multi-UAV-aided multi-active-IRS wireless communication network and a large-scale active IRS is split into K smaller distributed IRSs. There are M antennas in BS, where $M \geq K/K + 1$ and the user is equipped with N_u antennas, where $N_u \geq K/K + 1$. Besides, there are equipped with K small IRSs, each with

N_k reflective elements. Let us define $N_I = KN_k$, and N_I is the sum of numbers of all smaller IRS elements. The line-of-propagation channels are assumed in this paper.

The transmit baseband signal is

$$\mathbf{x} = \sum_{i=1}^{K} \mathbf{v}_i s_i, \tag{1}$$

where $\mathbf{v}_i \in \mathbb{C}^{M\times 1}$ is the i-th beamforming at BS with $\|\mathbf{v}_i\|^2 = 1$, and s_i is the i-th transmission symbol.

The reflect signal of the k-th IRS is

$$\mathbf{y}_k^t = \mathbf{\Theta}_k \mathbf{H}_k \mathbf{x} + \mathbf{\Theta}_k \mathbf{n}_k, \tag{2}$$

where $\mathbf{H}_k \in \mathbb{C}^{N_k\times M}$ denotes the transmission channel from the BS to the k-th IRS, and $\mathbf{\Theta}_k = \text{diag}(\alpha_1 e^{j\theta_1}, \ldots, \alpha_{N_k} e^{j\theta_{N_k}}) \in \mathbb{C}^{N_k\times N_k}$ stands for the reflection coefficient matrix of k-th IRS, where α_l represents amplitude gain and θ_l stands for phase shift, respectively. And $\mathbf{n}_k \in \mathbb{C}^{N_k\times 1}$ is the additive white Gaussian noise (AWGN) at IRS k, and $\mathbf{n}_k \sim \mathcal{CN}(0,\ \sigma_k^2 \mathbf{I}_{N_k})$.

The k-th signal at user is represented as

$$\mathbf{y}_k = \mathbf{G}_k^H \mathbf{\Theta}_k \mathbf{H}_k \mathbf{x} + \mathbf{G}_k^H \mathbf{\Theta}_k \mathbf{n}_k, \tag{3}$$

where $\mathbf{G}_k^H \in \mathbb{C}^{N_u\times N_k}$ denotes the channel from IRS k to user.

The total signal received at user is

$$\begin{aligned}\mathbf{y}_r &= \sum_{j=1}^{K} \mathbf{G}_j^H \mathbf{\Theta}_j \mathbf{H}_j \mathbf{x} + \sum_{j=1}^{K} \mathbf{G}_j^H \mathbf{\Theta}_j \mathbf{n}_j + \mathbf{z} \\ &= \sum_{j=1}^{K}\sum_{i=1}^{K} \mathbf{G}_j^H \mathbf{\Theta}_j \mathbf{H}_j \mathbf{v}_i s_i + \sum_{j=1}^{K} \mathbf{G}_j^H \mathbf{\Theta}_j \mathbf{n}_j + \mathbf{z}.\end{aligned} \tag{4}$$

The k-th data-stream signal of user is

$$\begin{aligned}y_k = \mathbf{u}_k^H \mathbf{y}_r &= \sum_{j=1}^{K}\sum_{i=1}^{K} \mathbf{u}_k^H \mathbf{G}_j^H \mathbf{\Theta}_j \mathbf{H}_j \mathbf{v}_i s_i \\ &+ \sum_{j=1}^{K} \mathbf{u}_k^H \mathbf{G}_j^H \mathbf{\Theta}_j \mathbf{n}_j + \mathbf{u}_k^H \mathbf{z},\end{aligned} \tag{5}$$

where $\mathbf{u}_k \in \mathbb{C}^{N_u\times 1}$ denotes the k-th receive beamforming vector with $\|\mathbf{u}_k\|^2 = 1$, and $\mathbf{z} \in \mathbb{C}^{N_u\times 1}$ is the AWGN at user, where $\mathbf{z} \sim \mathcal{CN}(0,\ \sigma_z^2 \mathbf{I}_{N_u})$.

B. VIEWING K SMALLER IRSS AS A LARGE VIRTUAL IRS

In Fig. 1(b), we view all of the distributed smaller IRSs as a virtual large-scale IRS. Here, the BS and user are still employed with M and N_u antennas, respectively.

Similarly, the total signal received at user is

$$\mathbf{y}_r = \mathbf{G}^H \mathbf{\Theta} \mathbf{H} \mathbf{V} \mathbf{s} + \mathbf{G}^H \mathbf{\Theta} \mathbf{n} + \mathbf{z}, \tag{6}$$

where $\mathbf{G}^H \in \mathbb{C}^{N_u\times N_I}$, $\mathbf{\Theta} \in \mathbb{C}^{N_I\times N_I}$ and $\mathbf{H} \in \mathbb{C}^{N_I\times M}$ respectively stand for the channel between this large-scale IRS with user, the PSM of IRS and the transmission channel from BS to IRS. $\mathbf{V} \in \mathbb{C}^{M\times K}$ denotes the transmit beamforming matrix. $\mathbf{s} \in \mathbb{C}^{K\times 1}$ is the transmission symbol vector. $\mathbf{n} \in \mathbb{C}^{N_I\times 1}$ is the AWGN of this large-scale IRS with distribution $\mathbf{n} \sim \mathcal{CN}(0,\ \sigma_n^2 \mathbf{I}_{N_I})$, where $\sigma_n^2 = K\sigma_k^2$.

Then, the total receive signal at user is rewritten as

$$\mathbf{y} = \mathbf{U}^H \mathbf{G}^H \mathbf{\Theta} \mathbf{H} \mathbf{V} \mathbf{s} + \mathbf{U}^H \mathbf{G}^H \mathbf{\Theta} \mathbf{n} + \mathbf{U}^H \mathbf{z}, \tag{7}$$

where $\mathbf{U}^H \in \mathbb{C}^{K\times N_u}$ denotes the receive beamforming matrix.

C. DOF ANALYSIS

Since there are K IRSs in the proposed multi-active IRS-aided DM network, a maximum of K DoFs is created. The specific derivation process is as follows

$$\text{rank}(\mathbf{H}) \le \min(M, K), \tag{8}$$

$$\text{rank}(\mathbf{G}) \le \min(K, N_u), \tag{9}$$

where

$$\mathbf{H} = \left[\mathbf{H}_1^H, \mathbf{H}_2^H, \ldots, \mathbf{H}_k^H, \ldots, \mathbf{H}_K^H\right]^H, \tag{10}$$

and

$$\mathbf{G} = \left[\mathbf{G}_1^H, \mathbf{G}_2^H, \ldots, \mathbf{G}_k^H, \ldots, \mathbf{G}_K^H\right]^H. \tag{11}$$

Then the DoF of our network can be written as

$$\text{DoF} \le \min(\text{rank}(\mathbf{H}), \text{rank}(\mathbf{G})) = \min(K, M, N_u). \tag{12}$$

Based on (12), the maximum DoF of our network is under the condition that all K smaller IRSs are randomly placed such that the K transmit steering vectors departing from BS are linear independence and form a basis of transmit signal space. Similarly, the K receive steering vectors impinging on receive array at user are also linear independence and forms a basis of the receive signal space. Thus, K parallel independent bit streams may be delivered from BS to user and it is necessary for us to set the $M \ge K/K + 1$ and $N_u \ge K/K + 1$. In this case, the maximum DoF of the system is K. Then the BS can transmit K data-streams simultaneously.

III. PROPOSED THREE METHODS

A. PROPOSED NSP-ZF-PA

To reduce the interference from other data-stream to the k-th data-stream signal, we project other stream interference information onto k-th null-space of transmission channel.

Define $\mathbf{H}_k \mathbf{v}_j = \mathbf{0}$, where $k \ne j$, then the k-th data-stream signal of user in (5) can be rewritten as

$$\begin{aligned}y_k &= \mathbf{u}_k^H \mathbf{G}_k^H \mathbf{\Theta}_k \mathbf{H}_k \mathbf{v}_k s_k + \sum_{j=1, j\ne k}^{K} \mathbf{u}_k^H \mathbf{G}_j^H \mathbf{\Theta}_j \mathbf{H}_j \mathbf{v}_j s_j \\ &+ \sum_{j=1}^{K} \mathbf{u}_k^H \mathbf{G}_j^H \mathbf{\Theta}_j \mathbf{n}_j + \mathbf{u}_k^H \mathbf{z},\end{aligned} \tag{13}$$

based on zero-forcing theorem, let $\mathbf{u}_i^H \mathbf{G}_k^H \to 0$, where $i \ne k$, then the power of k-th data-stream at user is given by

$$\mathbb{E}\left\{y_k^H y_k\right\} = \left|\mathbf{u}_k^H \mathbf{G}_k^H \mathbf{\Theta}_k \mathbf{H}_k \mathbf{v}_k s_k\right|^2 + \sum_{j=1}^{K} \sigma_j^2 \left\|\mathbf{u}_k^H \mathbf{G}_j^H \mathbf{\Theta}_j\right\|^2$$

$$+\sum_{j=1,j\neq k}^{K}\left|\mathbf{u}_k^H\mathbf{G}_j^H\boldsymbol{\Theta}_j\mathbf{H}_j\mathbf{v}_j s_j\right|^2+\sigma_z^2\left\|\mathbf{u}_k^H\right\|^2. \quad (14)$$

The SINR of the k-th data-stream is

$$\gamma_k=\frac{\left|\mathbf{u}_k^H\mathbf{G}_k^H\boldsymbol{\Theta}_k\mathbf{H}_k\mathbf{v}_k s_k\right|^2}{A}, \quad (15)$$

where

$$A=\sum_{j=1,j\neq k}^{K}\left|\mathbf{u}_k^H\mathbf{G}_j^H\boldsymbol{\Theta}_j\mathbf{H}_j\mathbf{v}_j s_j\right|^2+\sum_{j=1}^{K}\sigma_j^2\left\|\mathbf{u}_k^H\mathbf{G}_j^H\boldsymbol{\Theta}_j\right\|^2+\sigma_z^2\left\|\mathbf{u}_k^H\right\|^2. \quad (16)$$

As thus, the rate of user is written as

$$R_{m_1}=\sum_{k=1}^{K}\log_2(1+\gamma_k). \quad (17)$$

Next, let's focus on the specific design of transmit beamforming vector $\mathbf{v}_k$, receive beamforming vector $\mathbf{u}_k$ and the PSM $\boldsymbol{\Theta}_k$.

Let us define $\mathbf{H}_{-k}=[\mathbf{H}_1^H,\ldots,\mathbf{H}_{k-1}^H,\mathbf{H}_{k+1}^H,\ldots,\mathbf{H}_K^H]^H$, and fix $\mathbf{u}_k$, $\boldsymbol{\Theta}_k$, then the optimization problem with respect to $\mathbf{v}_k$ is presented as

$$\begin{aligned}\max_{\mathbf{v}_k}\quad & \mathbf{v}_k^H\mathbf{H}_k^H\mathbf{H}_k\mathbf{v}_k\\ \text{s.t.}\quad & \mathbf{H}_{-k}\mathbf{v}_k=\mathbf{0},\\ & \mathbf{v}_k^H\mathbf{v}_k=1.\end{aligned} \quad (18)$$

Define $\mathbf{T}_{-k}=[\mathbf{I}_M-\mathbf{H}_{-k}^H(\mathbf{H}_{-k}\mathbf{H}_{-k}^H)^\dagger\mathbf{H}_{-k}]$, and $\mathbf{v}_k=\mathbf{T}_{-k}\boldsymbol{\alpha}_k$, (18) can be converted as

$$\begin{aligned}\max_{\boldsymbol{\alpha}_k}\quad & \boldsymbol{\alpha}_k^H\mathbf{T}_{-k}^H\mathbf{H}_k^H\mathbf{H}_k\mathbf{T}_{-k}\boldsymbol{\alpha}_k\\ \text{s.t.}\quad & \boldsymbol{\alpha}_k^H\boldsymbol{\alpha}_k=1.\end{aligned} \quad (19)$$

Define $\mathbf{B}_k=\mathbf{T}_{-k}^H\mathbf{H}_k^H\mathbf{H}_k\mathbf{T}_{-k}$, noted that $\mathbf{B}_k$ is a Hermitian matrix, then it can be decomposed as

$$\mathbf{B}_k=\mathbf{E}_k\Lambda_1\mathbf{E}_k^H=\sum_{i=1}^{M}\lambda_i\mathbf{e}_i\mathbf{e}_i^H, \quad (20)$$

where $\Lambda_1=\mathrm{diag}(\lambda_1,\lambda_2,\ldots,\lambda_M)$, with $\lambda_1\leq\lambda_2\leq\cdots\leq\lambda_M$, according to the Rayleigh-Ritz theorem, we have $\boldsymbol{\alpha}_k=\mathbf{e}_M$.

Then the transmit beamforming vector is

$$\mathbf{v}_k=\frac{\mathbf{T}_{-k}\mathbf{e}_M}{\|\mathbf{T}_{-k}\mathbf{e}_M\|}. \quad (21)$$

Similarly, let $\mathbf{G}_{-k}=[\mathbf{G}_1^H,\ldots,\mathbf{G}_{k-1}^H,\mathbf{G}_{k+1}^H,\ldots,\mathbf{G}_K^H]$, and fix $\mathbf{v}_k$, $\boldsymbol{\Theta}_k$, then the optimization problem with respect to $\mathbf{u}_k$ is

$$\begin{aligned}\max_{\mathbf{u}_k}\quad & \mathbf{u}_k^H\mathbf{G}_k^H\mathbf{G}_k\mathbf{u}_k\\ \text{s.t.}\quad & \mathbf{u}_k^H\mathbf{G}_{-k}=\mathbf{0},\\ & \mathbf{u}_k^H\mathbf{u}_k=1.\end{aligned} \quad (22)$$

Define $\mathbf{L}_{-k}=[\mathbf{I}_{N_u}-\mathbf{G}_{-k}(\mathbf{G}_{-k}^H\mathbf{G}_{-k})^\dagger\mathbf{G}_{-k}^H]$, and $\mathbf{u}_k=\mathbf{L}_{-k}\boldsymbol{\zeta}_k$, (22) can be rewritten as

$$\begin{aligned}\max_{\boldsymbol{\zeta}_k}\quad & \boldsymbol{\zeta}_k^H\mathbf{L}_{-k}^H\mathbf{G}_k^H\mathbf{G}_k\mathbf{L}_{-k}\boldsymbol{\zeta}_k\\ \text{s.t.}\quad & \boldsymbol{\zeta}_k^H\boldsymbol{\zeta}_k=1.\end{aligned} \quad (23)$$

Let $\mathbf{C}_k=\mathbf{L}_{-k}^H\mathbf{G}_k^H\mathbf{G}_k\mathbf{L}_{-k}$, noted that $\mathbf{C}_k$ is also a Hermitian matrix, then it can be decomposed as

$$\mathbf{C}_k=\mathbf{F}_k\Lambda_2\mathbf{F}_k^H=\sum_{i=1}^{N_u}\mu_i\mathbf{f}_i\mathbf{f}_i^H, \quad (24)$$

where $\Lambda_2=\mathrm{diag}(\mu_1,\mu_2,\ldots,\mu_{N_u})$, and $\mu_1\leq\mu_2\leq\cdots\leq\mu_{N_u}$, according to the Rayleigh-Ritz theorem, we have $\boldsymbol{\zeta}_k=\mathbf{f}_{N_u}$.

Then the receive beamforming vector is shown as

$$\mathbf{u}_k=\frac{\mathbf{L}_{-k}\mathbf{f}_{N_u}}{\|\mathbf{L}_{-k}\mathbf{f}_{N_u}\|}. \quad (25)$$

The k-th useful signal power at user is

$$P_k=\mathbf{v}_k^H\mathbf{H}_k^H\boldsymbol{\Theta}_k^H\mathbf{G}_k\mathbf{u}_k\mathbf{u}_k^H\mathbf{G}_k^H\boldsymbol{\Theta}_k\mathbf{H}_k\mathbf{v}_k. \quad (26)$$

Let $\boldsymbol{\Theta}_k=\mathrm{diag}(\boldsymbol{\theta}_k)$, fixed $\mathbf{v}_k$ and $\mathbf{u}_k$, and define $\boldsymbol{\theta}_k=\tilde{\boldsymbol{\theta}}_k\tilde{\rho}_k$, where $\tilde{\rho}_k=\|\boldsymbol{\theta}_k\|$, $\tilde{\boldsymbol{\theta}}_k^H\tilde{\boldsymbol{\theta}}_k=1$. Based on the phase alignment (PA) theorem, the k-th useful signal power at user can be represented as

$$\begin{aligned}P_k&=\boldsymbol{\theta}_k^H\mathrm{diag}(\mathbf{H}_k\mathbf{v}_k)^H\mathbf{G}_k\mathbf{u}_k\mathbf{u}_k^H\mathbf{G}_k^H\mathrm{diag}(\mathbf{H}_k\mathbf{v}_k)\boldsymbol{\theta}_k\\&=\tilde{\rho}_k^2\tilde{\boldsymbol{\theta}}_k^H\mathrm{diag}(\mathbf{H}_k\mathbf{v}_k)^H\mathbf{G}_k\mathbf{u}_k\mathbf{u}_k^H\mathbf{G}_k^H\mathrm{diag}(\mathbf{H}_k\mathbf{v}_k)\tilde{\boldsymbol{\theta}}_k.\end{aligned} \quad (27)$$

Then the $\boldsymbol{\theta}_k$ can be obtained by

$$\boldsymbol{\theta}_k=\tilde{\boldsymbol{\theta}}_k\tilde{\rho}_k=\frac{\mathbf{u}_k^H\mathbf{G}_k^H\mathrm{diag}(\mathbf{H}_k\mathbf{v}_k)}{\|\mathbf{u}_k^H\mathbf{G}_k^H\mathrm{diag}(\mathbf{H}_k\mathbf{v}_k)\|}\tilde{\rho}_k. \quad (28)$$

The power reflected by the k-th IRS is

$$P_{I_k}=\tilde{\rho}_k^2\left(\left\|\mathrm{diag}(\mathbf{H}_k\mathbf{v}_k)\tilde{\boldsymbol{\theta}}_k^H\right\|^2+\sigma_k^2\right), \quad (29)$$

where P_{I_k} denotes the power budget at k small IRS, and

$$\tilde{\rho}_k=\sqrt{\frac{P_{I_k}}{\left\|\mathrm{diag}(\mathbf{H}_k\mathbf{v}_k)\tilde{\boldsymbol{\theta}}_k^H\right\|^2+\sigma_k^2}}. \quad (30)$$

B. PROPOSED WMMSE-PC

According to (7), the power of received signal at user is

$$\begin{aligned}\mathbb{E}\left\{\mathbf{y}\mathbf{y}^H\right\}&=\mathbf{U}^H\mathbf{G}^H\boldsymbol{\Theta}\mathbf{H}\mathbf{V}\mathbf{s}\mathbf{s}^H\mathbf{V}^H\mathbf{H}^H\boldsymbol{\Theta}^H\mathbf{G}\mathbf{U}\\&\quad+\sigma_n^2\mathbf{U}^H\mathbf{G}^H\boldsymbol{\Theta}\boldsymbol{\Theta}^H\mathbf{G}\mathbf{U}+\sigma_z^2\mathbf{U}^H\mathbf{U}.\end{aligned} \quad (31)$$

As thus, the final rate of user is

$$\begin{aligned}R_{m2}&=\log_2\left|\tilde{\mathbf{B}}^{-1}\left(\tilde{\mathbf{A}}+\tilde{\mathbf{B}}\right)\right|\\&=\log_2\left|\mathbf{I}_K+\frac{\tilde{\mathbf{A}}}{\tilde{\mathbf{B}}}\right|,\end{aligned} \quad (32)$$

where $\tilde{\mathbf{A}} = \mathbf{U}^H\mathbf{G}^H\mathbf{\Theta}\mathbf{H}\mathbf{V}\mathbf{s}\mathbf{s}^H\mathbf{V}^H\mathbf{H}^H\mathbf{\Theta}^H\mathbf{G}\mathbf{U}$, and $\tilde{\mathbf{B}} = \sigma_n^2\mathbf{U}^H\mathbf{G}^H\mathbf{\Theta}\mathbf{\Theta}^H\mathbf{G}\mathbf{U} + \sigma_z^2\mathbf{U}^H\mathbf{U}$.

Define $\mathbb{E}[\mathbf{s}\mathbf{s}^H] = \mathbf{I}_M$, and the total optimization problem can be expressed as

$$\begin{aligned} \max_{\mathbf{\Theta},\mathbf{V}} \quad & \log_2\left|\mathbf{I}_{N_u} + \frac{\mathbf{G}^H\mathbf{\Theta}\mathbf{H}\mathbf{V}\mathbf{V}^H\mathbf{H}^H\mathbf{\Theta}^H\mathbf{G}}{\sigma_n^2\mathbf{G}^H\mathbf{\Theta}\mathbf{\Theta}^H\mathbf{G} + \sigma_z^2\mathbf{I}_{N_u}}\right| \\ \text{s.t.} \quad & \|\mathbf{V}\|_F^2 \le P_B, \\ & \|\mathbf{\Theta}\mathbf{H}\mathbf{V}\mathbf{s}\|^2 + \|\mathbf{\Theta}\|_F^2\sigma_n^2 \le P_I. \end{aligned} \tag{33}$$

where P_B and P_I stand for the power budgets of BS and large-scale IRS, respectively.

Then, the mean-square error (MSE) of user is

$$\begin{aligned} \mathbf{E} &= \mathbb{E}\Big[(\mathbf{y}-\mathbf{s})(\mathbf{y}-\mathbf{s})^H\Big] \\ &= \Big(\mathbf{U}^H\mathbf{G}^H\mathbf{\Theta}\mathbf{H}\mathbf{V} - \mathbf{I}_K\Big)\Big(\mathbf{U}^H\mathbf{G}^H\mathbf{\Theta}\mathbf{H}\mathbf{V} - \mathbf{I}_K\Big)^H \\ &\quad + \sigma_n^2\mathbf{U}^H\mathbf{G}^H\mathbf{\Theta}\mathbf{\Theta}^H\mathbf{G}\mathbf{U} + \sigma_z^2\mathbf{U}^H\mathbf{U}, \end{aligned} \tag{34}$$

then (33) is converted as

$$\begin{aligned} \max_{\mathbf{W},\mathbf{U},\mathbf{\Theta},\mathbf{V}} \quad & h(\mathbf{W},\mathbf{U},\mathbf{\Theta},\mathbf{V}) \\ \text{s.t.} \quad & \|\mathbf{V}\|_F^2 \le P_B, \\ & \|\mathbf{\Theta}\mathbf{H}\mathbf{V}\mathbf{s}\|^2 + \|\mathbf{\Theta}\|_F^2\sigma_n^2 \le P_I, \end{aligned} \tag{35}$$

where

$$h(\mathbf{W},\mathbf{U},\mathbf{\Theta},\mathbf{V}) = \log_2|\mathbf{W}| - Tr(\mathbf{W}\mathbf{E}) + K, \tag{36}$$

where $\mathbf{W}$ is an auxiliary matrix. Now, the new problem is in a more tractable form [35].

Then given the first-order derivative function of $h(\mathbf{W},\mathbf{U},\mathbf{\Theta},\mathbf{V})$ with respect to $\mathbf{U}$ and make it equal zero, then the optimal $\mathbf{U}_{opt}$ is given by

$$\mathbf{U}_{opt} = \Big(\mathbf{G}^H\mathbf{\Theta}\mathbf{H}\mathbf{V}\mathbf{V}^H\mathbf{H}^H\mathbf{\Theta}^H\mathbf{G} + \tilde{\mathbf{C}}\Big)^{-1}\mathbf{G}^H\mathbf{\Theta}\mathbf{H}\mathbf{V}, \tag{37}$$

where $\tilde{\mathbf{C}} = \sigma_n^2\mathbf{G}^H\mathbf{\Theta}\mathbf{\Theta}^H\mathbf{G} + \sigma_z^2\mathbf{I}_{N_u}$.

Given $\mathbf{U}$, $\mathbf{\Theta}$ and $\mathbf{V}$, the optimal $\mathbf{W}$ is obtained as

$$\mathbf{W}_{opt} = \mathbf{E}^{-1}. \tag{38}$$

Now, let us focus on the optimizing of the $\mathbf{V}$ and $\mathbf{\Theta}$.

The optimization problem ($\mathbf{W}$, $\mathbf{U}$ and $\mathbf{\Theta}$ are fixed) with respect to $\mathbf{V}$ is given by

$$\begin{aligned} \min_{\mathbf{V}} \quad & Tr(\mathbf{W}\mathbf{E}) \\ \text{s.t.} \quad & \|\mathbf{V}\|_F^2 \le P_B, \\ & \|\mathbf{\Theta}\mathbf{H}\mathbf{V}\mathbf{s}\|^2 + \|\mathbf{\Theta}\|_F^2\sigma_n^2 \le P_I. \end{aligned} \tag{39}$$

It can be addressed by utilizing CVX packages, because (39) is a convex optimization problem.

The optimization problem ($\mathbf{W}$, $\mathbf{U}$ and $\mathbf{V}$ are fixed) with respect to $\mathbf{\Theta}$ is shown as

$$\begin{aligned} \min_{\mathbf{\Theta}} \quad & Tr\Big(\mathbf{\Theta}^H\hat{\mathbf{A}}\mathbf{\Theta}\hat{\mathbf{B}}\Big) + Tr\Big(\mathbf{\Theta}\hat{\mathbf{C}}\Big) + Tr\Big(\mathbf{\Theta}^H\hat{\mathbf{C}}^H\Big) \\ & + Tr\Big(\sigma_n^2\mathbf{\Theta}^H\hat{\mathbf{A}}\mathbf{\Theta}\Big) \\ \text{s.t.} \quad & \|\mathbf{\Theta}\mathbf{H}\mathbf{V}\mathbf{s}\|^2 + \|\mathbf{\Theta}\|_F^2\sigma_n^2 \le P_I, \end{aligned} \tag{40}$$

where $\hat{\mathbf{A}} = \mathbf{G}\mathbf{U}\mathbf{W}\mathbf{U}^H\mathbf{G}^H$, $\hat{\mathbf{B}} = \mathbf{H}\mathbf{V}\mathbf{V}^H\mathbf{H}^H$, $\hat{\mathbf{C}} = -\mathbf{H}\mathbf{V}\mathbf{W}\mathbf{U}^H\mathbf{G}^H$. Based on [35], the optimization problem (40) is converted to

$$\begin{aligned} \min_{\boldsymbol{\theta}} \quad & f(\boldsymbol{\theta}) = \boldsymbol{\theta}^H\Omega\boldsymbol{\theta} + 2Re\Big\{\boldsymbol{\theta}^H\mathbf{c}^*\Big\} \\ \text{s.t.} \quad & \|\mathbf{\Theta}\mathbf{H}\mathbf{V}\mathbf{s}\|^2 + \|\mathbf{\Theta}\|_F^2\sigma_n^2 \le P_I, \end{aligned} \tag{41}$$

where $\mathbf{\Theta} = \mathrm{diag}(\boldsymbol{\theta})$, $\mathbf{C} = \mathrm{diag}(\mathbf{c})$ and $\Omega = \hat{\mathbf{A}}\odot\hat{\mathbf{B}}^T + \sigma_n^2\hat{\mathbf{A}}\odot\mathbf{I}$.

Then the majorization-minimization (MM) algorithm is utilized to figure out (41).

Noted that

$$\begin{aligned} \boldsymbol{\theta}^H\Omega\boldsymbol{\theta} \le{}& \boldsymbol{\theta}^H\mathbf{X}\boldsymbol{\theta} - 2Re\Big\{\boldsymbol{\theta}^H(\mathbf{X}-\Omega)\boldsymbol{\theta}^t\Big\} \\ & + \big(\boldsymbol{\theta}^t\big)^H(\mathbf{X}-\Omega)\boldsymbol{\theta}^t = \hat{f}\big(\boldsymbol{\theta}|\boldsymbol{\theta}^t\big), \end{aligned} \tag{42}$$

where $\boldsymbol{\theta}^t$ is the value of $\boldsymbol{\theta}$ after t iterations, and $\mathbf{X} = \lambda_{max}(\Omega)\mathbf{I}$, λ_{max} is the maximum eigenvalue of Ω, then the upper bound function of $f(\boldsymbol{\theta})$ is

$$g\big(\boldsymbol{\theta}|\boldsymbol{\theta}^t\big) = \hat{f}\big(\boldsymbol{\theta}|\boldsymbol{\theta}^t\big) + 2Re\Big\{\boldsymbol{\theta}^H\mathbf{c}^*\Big\}. \tag{43}$$

Let us define $P_I = \|\mathbf{\Theta}\mathbf{H}\mathbf{V}\mathbf{s}\|^2 + \|\mathbf{\Theta}\|_F^2\sigma_n^2$, and $\boldsymbol{\theta} = \gamma\tilde{\boldsymbol{\theta}}$, where $\tilde{\boldsymbol{\theta}}^H\tilde{\boldsymbol{\theta}} = KN_k$, (41) is transformed as

$$\begin{aligned} \max_{\tilde{\boldsymbol{\theta}}} \quad & 2Re\Big\{\gamma\tilde{\boldsymbol{\theta}}^H\mathbf{q}^t\Big\} \\ \text{s.t.} \quad & |\tilde{\theta}_s| = 1, \end{aligned} \tag{44}$$

where

$$\gamma = \sqrt{\frac{P_I}{\Big\|\tilde{\mathbf{\Theta}}\mathbf{H}\mathbf{V}\mathbf{s}\Big\|^2 + \Big\|\tilde{\mathbf{\Theta}}\Big\|_F^2\sigma_n^2}}, \tag{45}$$

and $\tilde{\theta}_s$ is the s-th element of $\tilde{\boldsymbol{\theta}}$, $\tilde{\mathbf{\Theta}} = \mathrm{diag}(\tilde{\boldsymbol{\theta}})$ and $\mathbf{q}^t = (\lambda_{max}\mathbf{I} - \Omega)\gamma\tilde{\boldsymbol{\theta}}^t - \mathbf{c}^*$. Then the optimal solution of (41) is shown as

$$\boldsymbol{\theta}^{t+1} = \gamma e^{jarg(\mathbf{q}^t)}, \tag{46}$$

For a clearer presentation of MM algorithm, its specific procedure is listed in the following Algorithm 1.

Algorithm 1 MM Algorithm

1: Initial t=1, $\tilde{\boldsymbol{\theta}}^0$, error tolerance $\epsilon = 10^{-6}$. And acquire the value of $f(\boldsymbol{\theta}^1)$ in (41);
2: Calculate $\mathbf{q}^t = (\lambda_{max}\mathbf{I} - \Omega)\gamma\tilde{\boldsymbol{\theta}}^t - \mathbf{c}^*$ and Update $\boldsymbol{\theta}^{t+1}$ based on (46);
3: Calculate $f(\boldsymbol{\theta}^{t+1})$, if $|f(\boldsymbol{\theta}^{t+1}) - f(\boldsymbol{\theta}^t)|/f(\boldsymbol{\theta}^{t+1}) \le \epsilon$ holds, end loop; If not, back to step 2.

The details of entire algorithm about proposed WMMSE-PC is shown in Algorithm 2. Noticed that the objective function of (33) is limited to the finite value under the power constraints, which implied that the Algorithm 2 can ensure convergence.

Algorithm 2 The Proposed WMMSE-PC Algorithm

1: Initial s=1, the maximum number of iterations s_{max} = 200, error tolerance ϵ. Input the initialization $\mathbf{V}^{(1)}$, $\mathbf{\Theta}^{(1)}$, calculate the value of (33) and represented as $Obj(\mathbf{V}^{(1)}, \mathbf{\Theta}^{(1)})$;
2: Fixed $\mathbf{V}^{(s)}$, $\mathbf{\Theta}^{(s)}$, obtain $\mathbf{U}^{(s)}$ in (37);
3: Fixed $\mathbf{V}^{(s)}$, $\mathbf{\Theta}^{(s)}$ and $\mathbf{U}^{(s)}$, calculate $\mathbf{W}^{(s)}$ in (38);
4: Fixed $\mathbf{W}^{(s)}$, $\mathbf{\Theta}^{(s)}$ and $\mathbf{U}^{(s)}$, obtain $\mathbf{V}^{(s+1)}$ by solving problem (39);
5: Fixed $\mathbf{W}^{(s)}$, $\mathbf{U}^{(s)}$ and $\mathbf{V}^{(s+1)}$, calculate $\mathbf{\Theta}^{(s+1)}$ by working out problem (40);
6: if $s \geq s_{max}$ or $|Obj(\mathbf{V}^{(s+1)}, \mathbf{\Theta}^{(s+1)}) - Obj(\mathbf{V}^{(s)}, \mathbf{\Theta}^{(s)})|/Obj(\mathbf{V}^{(s)}, \mathbf{\Theta}^{(s)}) < \epsilon$, end loop. If not, back to step 2.

C. PROPOSED MAX-TR-SVD

Based on (33), the overall optimization problem in proposed Max-TR-SVD can be expressed as

$$\begin{aligned} \max_{\mathbf{\Theta},\mathbf{V}} \ & \mathbf{G}^H\mathbf{\Theta}\mathbf{H}\mathbf{V}\mathbf{s}\mathbf{s}^H\mathbf{V}^H\mathbf{H}^H\mathbf{\Theta}^H\mathbf{G} \\ \text{s.t.} \ & \|\mathbf{V}\|_F^2 \leq P_B, \\ & \|\mathbf{\Theta}\mathbf{H}\mathbf{V}\mathbf{s}\|^2 + \|\mathbf{\Theta}\|_F^2\sigma_n^2 \leq P_I. \end{aligned} \tag{47}$$

According to SVD theorem

$$\mathbf{H} = \mathbf{U}_1\Sigma_1\mathbf{V}_1^H, \tag{48}$$

and

$$\mathbf{G}^H = \mathbf{U}_2\Sigma_2\mathbf{V}_2^H, \tag{49}$$

then the transmit beamforming $\mathbf{V}$ and receive beamforming $\mathbf{U}$ are obtained from $\mathbf{V}_1$ and $\mathbf{U}_2$, respectively.

(47) can be converted to

$$\begin{aligned} \max_{\mathbf{\Theta}} \ & tr\left(\mathbf{G}^H\mathbf{\Theta}\mathbf{H}\mathbf{V}\mathbf{s}\mathbf{s}^H\mathbf{V}^H\mathbf{H}^H\mathbf{\Theta}^H\mathbf{G}\right) \\ \text{s.t.} \ & \|\mathbf{\Theta}\mathbf{H}\mathbf{V}\mathbf{s}\|^2 + \|\mathbf{\Theta}\|_F^2\sigma_n^2 \leq P_I. \end{aligned} \tag{50}$$

Define $\mathbf{\Theta} = \text{diag}(\boldsymbol{\theta})$, (50) can be rewritten as

$$\begin{aligned} \max_{\boldsymbol{\theta}} \ & \boldsymbol{\theta}^H\text{diag}(\mathbf{H}\mathbf{V}\mathbf{s})^H\mathbf{G}\mathbf{G}^H\text{diag}(\mathbf{H}\mathbf{V}\mathbf{s})\boldsymbol{\theta} \\ \text{s.t.} \ & \boldsymbol{\theta}^H\left(\text{diag}(\mathbf{H}\mathbf{V}\mathbf{s})^H\text{diag}(\mathbf{H}\mathbf{V}\mathbf{s}) + \sigma_n^2\mathbf{I}\right)\boldsymbol{\theta} \leq P_I. \end{aligned} \tag{51}$$

Let us define $P_I = \boldsymbol{\theta}^H(\text{diag}(\mathbf{H}\mathbf{V}\mathbf{s})^H\text{diag}(\mathbf{H}\mathbf{V}\mathbf{s}) + \sigma_n^2\mathbf{I})\boldsymbol{\theta}$, and $\boldsymbol{\theta} = \hat{\rho}\hat{\boldsymbol{\theta}}$, where $\hat{\rho} = \|\boldsymbol{\theta}\|$, $\hat{\boldsymbol{\theta}}^H\hat{\boldsymbol{\theta}} = 1$, then the (51) can be rewritten as

$$\max_{\hat{\boldsymbol{\theta}}} \ \frac{\hat{\boldsymbol{\theta}}^H\text{diag}(\mathbf{H}\mathbf{V}\mathbf{s})^H\mathbf{G}\mathbf{G}^H\text{diag}(\mathbf{H}\mathbf{V}\mathbf{s})\hat{\boldsymbol{\theta}}}{\hat{\boldsymbol{\theta}}^H\frac{1}{P_I}\left(\text{diag}(\mathbf{H}\mathbf{V}\mathbf{s})^H\text{diag}(\mathbf{H}\mathbf{V}\mathbf{s}) + \sigma_n^2\mathbf{I}\right)\hat{\boldsymbol{\theta}}}, \tag{52}$$

where $\hat{\boldsymbol{\theta}}$ is the eigenvector corresponding to the maximum eigenvalue of $\hat{\mathbf{D}}$, where

$$\hat{\mathbf{D}} = \frac{\text{diag}(\mathbf{H}\mathbf{V}\mathbf{s})^H\mathbf{G}\mathbf{G}^H\text{diag}(\mathbf{H}\mathbf{V}\mathbf{s})}{\frac{1}{P_I}\left(\text{diag}(\mathbf{H}\mathbf{V}\mathbf{s})^H\text{diag}(\mathbf{H}\mathbf{V}\mathbf{s}) + \sigma_n^2\mathbf{I}\right)}. \tag{53}$$

Then

$$\hat{\rho} = \sqrt{\frac{P_I}{\hat{\boldsymbol{\theta}}^H\left(\text{diag}(\mathbf{H}\mathbf{V}\mathbf{s})^H\text{diag}(\mathbf{H}\mathbf{V}\mathbf{s}) + \sigma_n^2\mathbf{I}\right)\hat{\boldsymbol{\theta}}}}, \tag{54}$$

then the $\boldsymbol{\theta} = \hat{\rho}\hat{\boldsymbol{\theta}}$, and $\mathbf{\Theta} = \text{diag}(\boldsymbol{\theta})$.

IV. PERFORMANCE AND COMPLEXITY ANALYSIS

A. WHEN $P_I \to \infty$

In this section, when P_B is fixed, while increasing P_I, we make an analysis about the performance.

Based on (15), the SINR of k-th data-stream is

$$\gamma_k = \frac{\frac{P_B}{K}P_{I_k}A_1}{\frac{P_B}{K}\sum_{j=1,j\neq k}^{K}P_{I_j}A_2 + P_{I_k}A_3 + \sum_{j=1,j\neq k}^{K}P_{I_j}A_4 + \sigma_z^2\left\|\mathbf{u}_k^H\right\|^2}, \tag{55}$$

where

$$A_1 = \frac{\left\|\mathbf{u}_k^H\mathbf{G}_k^H\right\|^2\left\|\text{diag}\left(\tilde{\boldsymbol{\theta}}_k\right)\right\|^2\|\mathbf{H}_k\mathbf{v}_k s_k\|^2}{\left\|\text{diag}(\mathbf{H}_k\mathbf{v}_k)\tilde{\boldsymbol{\theta}}_k\right\|^2 + \sigma_k^2}, \tag{56}$$

$$A_2 = \frac{\left\|\mathbf{u}_k^H\mathbf{G}_j^H\right\|^2\left\|\text{diag}\left(\tilde{\boldsymbol{\theta}}_j\right)\right\|^2\left\|\mathbf{H}_j\mathbf{v}_j s_j\right\|^2}{\left\|\text{diag}\left(\mathbf{H}_j\mathbf{v}_j\right)\tilde{\boldsymbol{\theta}}_j\right\|^2 + \sigma_j^2}, \tag{57}$$

$$A_3 = \frac{\sigma_k^2\left\|\mathbf{u}_k^H\mathbf{G}_k^H\right\|^2\left\|\text{diag}\left(\tilde{\boldsymbol{\theta}}_k\right)\right\|^2}{\left\|\text{diag}(\mathbf{H}_k\mathbf{v}_k)\tilde{\boldsymbol{\theta}}_k\right\|^2 + \sigma_k^2}, \tag{58}$$

$$A_4 = \frac{\sigma_j^2\left\|\mathbf{u}_k^H\mathbf{G}_j^H\right\|^2\left\|\text{diag}\left(\tilde{\boldsymbol{\theta}}_j\right)\right\|^2}{\left\|\text{diag}\left(\mathbf{H}_j\mathbf{v}_j\right)\tilde{\boldsymbol{\theta}}_j\right\|^2 + \sigma_j^2}. \tag{59}$$

Noted that when $i \neq k$, the $\mathbf{u}_i^H\mathbf{G}_k^H \to 0$, we have A_2 and A_4 are $\to 0$. At this point, (55) can be rewritten as

$$\gamma_k = \frac{\frac{P_B}{K}P_{I_k}A_1}{P_{I_k}A_3 + \sigma_z^2\|\mathbf{u}_k^H\|^2}. \tag{60}$$

When $P_I \to \infty$ and all other elements are fixed, then $P_{I_k} \to \infty$, finally we have

$$\gamma_k = \frac{P_B A_1}{KA_3}. \tag{61}$$

We can find that it is a constant, which means the achievable rate will reach to a platform period with a continuous increases in the value of P_I.

Similar to the derivation of (61), we can convert (32) to

$$R_{m2} = \log_2\left|\mathbf{I}_K + \frac{P_I\mathbf{Q_1}}{P_I\mathbf{Q_2} + \sigma_z^2\mathbf{U}^H\mathbf{U}}\right|, \tag{62}$$

where

$$\mathbf{Q_1} = \frac{\mathbf{U}^H\mathbf{G}^H\tilde{\mathbf{\Theta}}\mathbf{H}\mathbf{V}\mathbf{s}\mathbf{s}^H\mathbf{V}^H\mathbf{H}^H\tilde{\mathbf{\Theta}}^H\mathbf{G}\mathbf{U}}{\left\|\tilde{\mathbf{\Theta}}\mathbf{H}\mathbf{V}\mathbf{s}\right\|^2 + \left\|\tilde{\mathbf{\Theta}}\right\|_F^2\sigma_n^2}, \tag{63}$$

$$\mathbf{Q_2} = \frac{\sigma_n^2 \mathbf{U}^H \mathbf{G}^H \tilde{\mathbf{\Theta}} \tilde{\mathbf{\Theta}}^H \mathbf{G} \mathbf{U}}{\left\|\tilde{\mathbf{\Theta}} \mathbf{H} \mathbf{V} \mathbf{s}\right\|^2 + \left\|\tilde{\mathbf{\Theta}}\right\|_F^2 \sigma_n^2}. \tag{64}$$

When $P_I \to \infty$ and all other elements are fixed, (62) reduces to

$$R_{m2} = \log_2 \left| \mathbf{I}_K + \frac{\mathbf{Q_1}}{\mathbf{Q_2}} \right|, \tag{65}$$

which is also a constant.

B. THE RELATIONSHIP BETWEEN γ_0 AND γ_U

In this section, the impact of average SINR at the k-th active IRS on the k data-stream receive SINR at the user will be shown.

The receive signal about the n-th element at IRS k is recast as

$$y_n = \mathbf{h}_k^H(n) \sum_{j=1}^{K} \mathbf{v}_j s_j + w_i(n), \tag{66}$$

where $\mathbf{h}_k(n) \in \mathbb{C}^{M \times 1}$ denotes the transmission channel from the BS to the n-th component element of IRS k. $w_i(n)$ is the AWGN at the n-th component element of IRS k and $w_i(n) \sim \mathcal{CN}(0,\ \sigma_i^2)$.

Since $k \neq j$, $\mathbf{H}_k \mathbf{v}_j = \mathbf{0}$, then $\mathbf{h}_k^H(n)\mathbf{v}_j = 0$, (66) can be converted as

$$y_n = \mathbf{h}_k^H(n) \mathbf{v}_k s_k + w_i(n). \tag{67}$$

Then the average SINR at k-th IRS is

$$\gamma_0 = \frac{P_B \sum_{n=1}^{N_k} \left| \mathbf{h}_k^H(n) \mathbf{v}_k \right|^2}{N_k \sigma_i^2}. \tag{68}$$

The k-th data stream receive signal based on (13) at user may be expressed in the vector form

$$\begin{aligned} y_u = & \sum_{n=1}^{N_k} \mathbf{u}_k^H \mathbf{g}_k(n) \varphi_k(n) \mathbf{h}_k^H(n) \mathbf{v}_k s_k \\ & + \sum_{n=1}^{N_k} \mathbf{u}_k^H \mathbf{g}_k(n) \varphi_k(n) w_i(n) \\ & + \sum_{n=1}^{N_k} \sum_{j=1, j\neq k}^{K} \mathbf{u}_k^H \mathbf{g}_j(n) \varphi_j(n) \mathbf{h}_j^H(n) \mathbf{v}_j s_j \\ & + \sum_{n=1}^{N_k} \sum_{j=1, j\neq k}^{K} \mathbf{u}_k^H \mathbf{g}_j(n) \varphi_j(n) w_i(n) + \mathbf{u}_k^H \mathbf{z}, \end{aligned} \tag{69}$$

where $\mathbf{g}_k(n) \in \mathbb{C}^{N_u \times 1}$ stands for the channel from the n-th element of IRS k to user, $\varphi_k(n)$ is the n-th element of $\mathbf{\Theta}_k$. Similarly, when $i \neq k$, $\mathbf{u}_i^H \mathbf{G}_k^H \to \mathbf{0}$, then $\mathbf{u}_i^H \mathbf{g}_j(n) \to 0$, then (69) is simplified as

$$\begin{aligned} y_u = & \sum_{n=1}^{N_k} \mathbf{u}_k^H \mathbf{g}_k(n) \varphi_k(n) \mathbf{h}_k^H(n) \mathbf{v}_k s_k \\ & + \sum_{n=1}^{N_k} \mathbf{u}_k^H \mathbf{g}_k(n) \varphi_k(n) w_i(n) + \mathbf{u}_k^H \mathbf{z}. \end{aligned} \tag{70}$$

Then we can acquire the power of the k-th data-stream receive signal at user is

$$\begin{aligned} \mathbb{E}\left\{ y_u^H y_u \right\} = & \sum_{n=1}^{N_k} \left| \mathbf{u}_k^H \mathbf{g}_k(n) \varphi_k(n) \mathbf{h}_k^H(n) \mathbf{v}_k \right|^2 \\ & + \sum_{n=1}^{N_k} \sigma_i^2 \left| \mathbf{u}_k^H \mathbf{g}_k(n) \varphi_k(n) \right|^2 + \sigma_z^2 \left\| \mathbf{u}_k^H \right\|^2. \end{aligned} \tag{71}$$

The signal reflected through the n-th reflect element of k-th small IRS is

$$y_i(n) = \varphi_k(n) \mathbf{h}_k^H(n) \mathbf{v}_k s_k + \varphi_k(n) w_i(n). \tag{72}$$

The average total power of all N_k elements of k-th small IRS is

$$P_{I_k} = P_B \sum_{n=1}^{N_k} \left| \varphi_k(n) \mathbf{h}_k^H(n) \mathbf{v}_k \right|^2 + \sigma_i^2 \sum_{n=1}^{N_k} |\varphi_k(n)|^2. \tag{73}$$

Let us define

$$|\varphi_k(n)| = \lambda_k = \sqrt{\frac{P_{I_k}}{P_B \sum_{n=1}^{N_k} \left| \mathbf{h}_k^H(n) \mathbf{v}_k \right|^2 + \sigma_i^2 N_k}}. \tag{74}$$

The SINR of k-th data stream receive signal at user is

$$\gamma_u = \frac{P_B \sum_{n=1}^{N_k} \left| \mathbf{u}_k^H \mathbf{g}_k(n) \varphi_k(n) \mathbf{h}_k^H(n) \mathbf{v}_k \right|^2}{\sum_{n=1}^{N_k} \sigma_i^2 \left| \mathbf{u}_k^H \mathbf{g}_k(n) \varphi_k(n) \right|^2 + \sigma_z^2 \left\| \mathbf{u}_k^H \right\|^2}. \tag{75}$$

Then substituting (74) in (75), and when $P_I \to \infty$, we can transform (75) to

$$\gamma_u = \frac{P_B \sum_{n=1}^{N_k} \left| \mathbf{u}_k^H \mathbf{g}_k(n) \mathbf{h}_k^H(n) \mathbf{v}_k \right|^2}{\sigma_i^2 \sum_{n=1}^{N_k} \left| \mathbf{u}_k^H \mathbf{g}_k(n) \right|^2}. \tag{76}$$

According to (68) and (76), the relationship between the γ_u and the γ_0 is shown as

$$\gamma_u = C_1 \gamma_0, \tag{77}$$

where

$$C_1 = \frac{E\left[\left| \mathbf{u}_k^H \mathbf{g}_k(n) \mathbf{h}_k^H(n) \mathbf{v}_k \right|^2 \right]}{E\left[\left| \mathbf{u}_k^H \mathbf{g}_k(n) \right|^2 \right] E\left[\left| \mathbf{h}_k^H(n) \mathbf{v}_k \right|^2 \right]}. \tag{78}$$

It can be found that the receive SINR at user of k-th data-stream is proportional to γ_0 when N_k is fixed. When reducing the noise at IRS elements or increasing the transmit power P_B, the receive SINR at user grows linearly.

The complexity of proposed three methods are shown as follows. Their complexity is expressed as a growing order (floating point operations per second (FLOPs)): Max-TR-SVD ($\mathcal{O}(K^3 N_k^3 + N_u K^2 N_k^2 + K M^2 N_k)$ FLOPs), NSP-ZF-PA ($\mathcal{O}(K(2K^3 N_k^3 + N_k^2))$ FLOPs), WMMSE-PC ($\mathcal{O}(L_1(K^{3.5} N_k^{3.5} + L_2 K^3 N_k^3 + 2K^3))$ FLOPs), where L_1 and L_2 denote the iteration numbers of WMMSE-PC and MM, respectively.

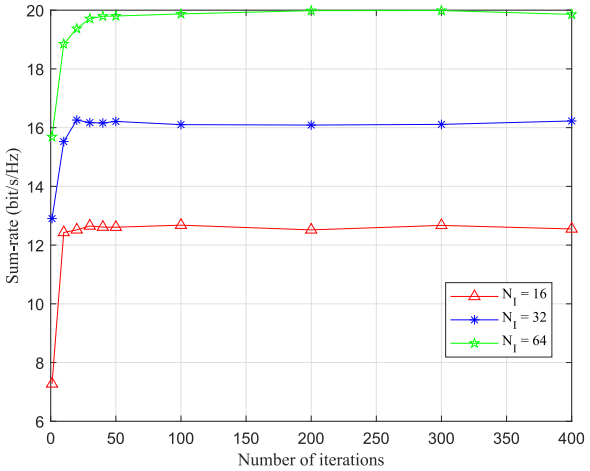

FIGURE 2. Convergence behavior of WMMSE-PC.

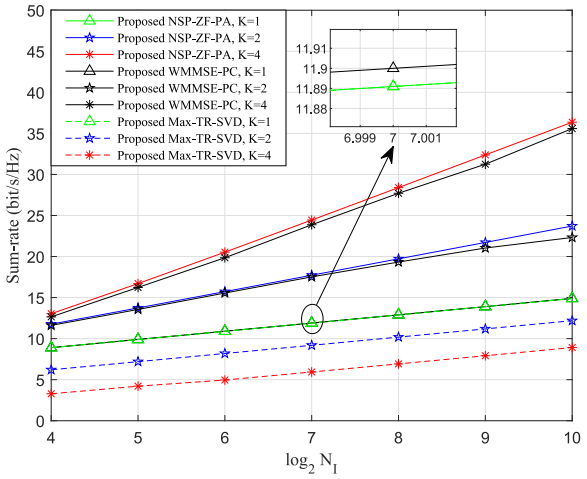

FIGURE 3. Sum-rate versus N_I.

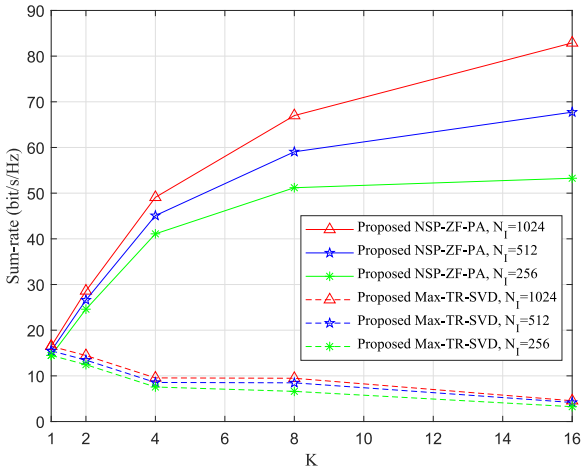

FIGURE 4. Sum-rate versus number of IRSs K.

V. SIMULATION RESULTS

In what follows, simulation are presented to assess the convergence and the sum-rate of the proposed three methods. The parameters of simulation are set as: $\sigma_k^2 = \sigma_z^2 = -40$ dBm, $P_B = 30$ dBm, $P_I = 0.04$ W. $M = N_u = 8$. The coefficient of path loss is chosen as: $l_0 = \alpha/d_0^c$, where $c = 2$, $\alpha = 10^{-2}$ and d_0 represents the reference distance. The BS and user are at the original point (0m, 0m) and (100m, 0m), respectively. When there is one large-scale IRS, it is located at (80m, 20m); when there are two small IRSs, it is located at (80m, 20m) and (90m, 30m); when there are four small IRSs, it is located at (80m, 20m), (90m, 30m), (80m, −20m) and (90m, −30m).

Fig. 2 demonstrates the convergence behavior of the proposed WMMSE-PC. It is clearly found that the sum-rate converges fast within fifty iterations with four small IRSs, where the number of the total IRS elements $N_I = 16$, 32 and 64. The achieved rate increases with N_I. Additionally, the WMMSE-PC has a similar convergence speed regardless of the value of N_I.

Fig. 3 depicts the sum-rate versus the entire number of active IRS reflecting elements N_I for the three different methods proposed by us. The proposed NSP-ZF-PA and WMMSE-PC have achieved significant rate enhancement over Max-TR-SVD. More importantly, when $K = 2$ and $K = 4$, the rates of the proposed NSP-ZF-PA and WMMSE-PC are about 1.6 and 2.4 times that with $K = 1$ when $N_I = 1024$. That is mainly due to the fact that the maximum DoF increases when there are more IRSs. According to (12), the maximum DoF is four when $K = 4$, and there were four data-streams transmitted simultaneously. Thus, we make a conclusion that increasing the number of IRSs with a fixed total number of all IRS elements will have a dominant impact on the performance of rate. This will be further confirmed in the next figure. In other words, a more IRSs means a larger DoF and a higher rate.

Fig. 4 demonstrates the sum-rate versus K, which is total number of IRSs, where $M = N_u = 24$. As the value of K ranges from 1, 2, 4, 8 and 16, the rate of NSP-ZF-PA with sixteen distributed IRSs is about 5 times that of NSP-ZF-PA with combining all small IRSs as a single large IRS when $N_I = 1024$, and about 4.4 times when $N_I = 512$, and about 3.7 times when $N_I = 256$. This is mainly due to the fact that the DoF of network increases from 1 to 16. The transmission data-streams also increases from 1 to 16, and it can be transmitted independence among the different data-stream. It can achieve a significant enhancement in this case based on (17).

Fig. 5 demonstrates the sum-rate versus the sum power P_I at IRS for the proposed three methods given transmit power $P_B = 30$ dBm at BS, where the sum number of IRS $N_I = 64, 256$, $K = 4$. It can be seen that the proposed NSP-ZF-PA and WMMSE-PC first grow as $P_I \leq 20$ dBm increases, but finally reaches a rate ceil when $P_I \geq 20$ dBm. When $P_I \to \infty$, the achievable rate turns into a constant, which is consistent with the previous conclusions of (61) and (65). This result implies that give a fixed transmit power, there is an optimal minimum power budget at IRS to make a highest rate, i.e., the rate upper bound. Placing more power

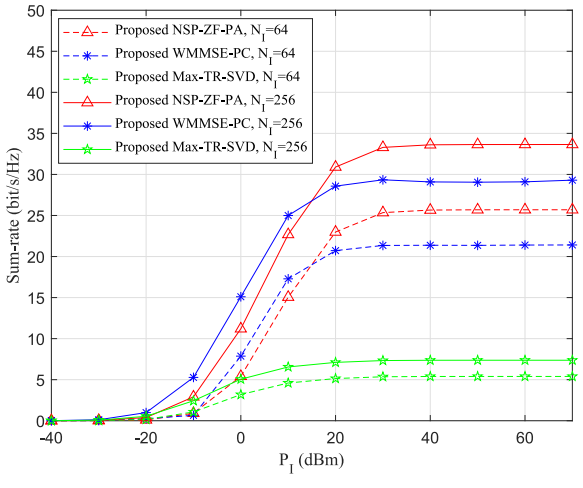

FIGURE 5. Sum-rate versus P_I.

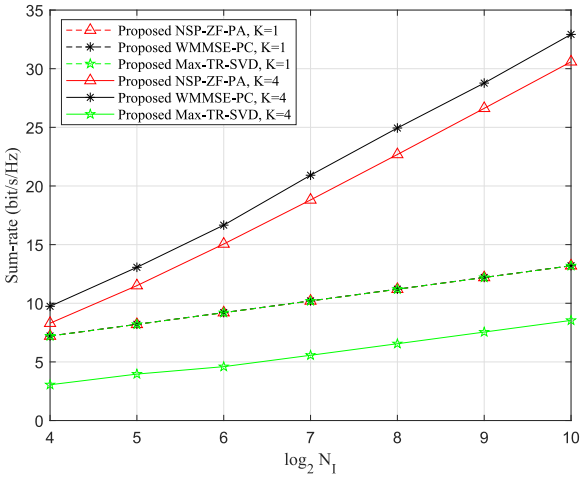

FIGURE 6. Achieved sum-rate when $P_I = 10$ dBm.

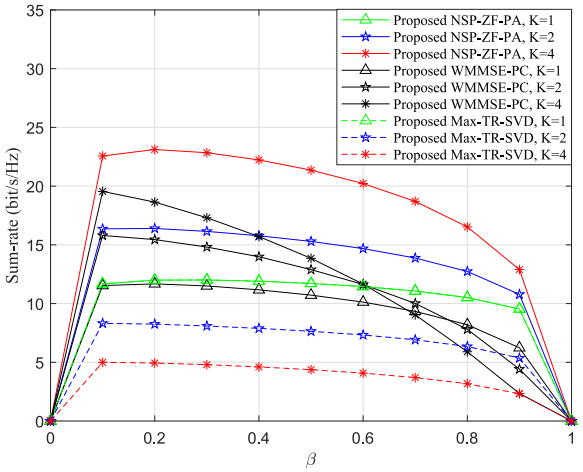

FIGURE 7. Sum-rate versus the power allocation factor β.

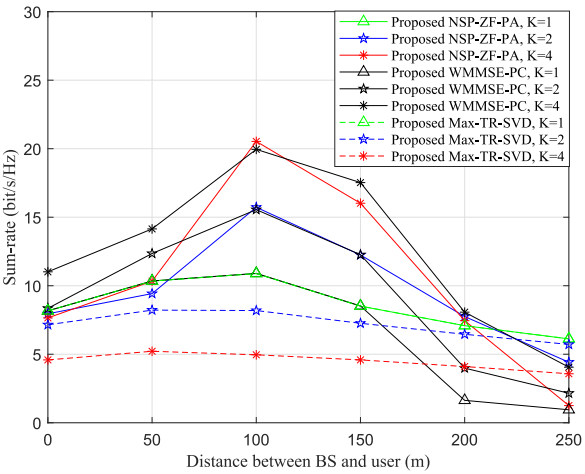

FIGURE 8. Sum-rate versus the linear distance between BS and USER.

on IRS will waste power. The main reason for this tendency is the effect of noise accumulation at IRS.

Fig. 6 shows the sum-rates of NSP-ZF-PA and WMMSE-PC versus the total number N_I of IRS elements with $P_I = 10$ dBm for two different values of K. When $K = 4$, the rate performance of WMMSE-PC is better than NSP-ZF-PA. This result is converse to that in Fig. 3. However, the rate growing tendency of both methods is similar to those in the previous figures.

Fig. 7 depicts the sum-rate versus the PA factor β under the total power constraint of $P_T = 1$ W, where the power of all IRSs $P_I = \beta P_T$, and $N_I = 64$. $\beta = 0.1$ means $P_I = 0.1$ W. When $K = 1$, it can be observed that the optimal PA factor value of β of the proposed NSP-ZF-PA, the WMMSE-PC and Max-TR-SVD approach zero as the number K of IRSs increases. This means less power is allocated to the IRSs.

Fig. 8 plots the sum-rate versus the distance between BS and user, where $N_I = 64$. It can be shown from Fig. 8 that there is a peak value of proposed NSP-ZF-PA and WMMSE-PC when the distance between BS and user is 100m. That is because at this point, the IRS is very close to user, i.e., the distance from IRS to user is zero, and can harvest more performance gain. When the distance of BS and user $\geq$ 100 m, the sum-rates of proposed NSP-ZF-PA and WMMSE-PC reduce as the distance between BS and user increases, due to the increase in path loss.

VI. CONCLUSION

In this paper, a novel multi-IRS-aided multi-stream DM network was investigated. This network may form a high K ($\geq$ 3) DoFs to achieve a point-to-point multi-stream by utilizing the distributed small IRSs on UAVs. Subsequently, three high-performance methods, called NSP-ZF-PA, WMMSE-PC, and Max-TR-SVD, were proposed and the computational complexities of these methods were also compared. Simulation results verified their rates. Particularly, the rate of NSP-ZF-PA with sixteen distributed IRSs was about five times that of NSP-ZF-PA with combining all small IRSs as a single large IRS. The proposed NSP-ZF-PA

and WMMSE-PC performed much better than Max-TR-SVD for multiple-IRS scenario in terms of rate. However, the Max-TR-SVD has the lowest complexity. And the rate of NSP-ZF-PA is better than that of WMMSE-PC under the large power budget of IRS, and is worse than that of WMMSE-PC under the low power budget of IRS.

REFERENCES

[1] R. Liu, R. Yu-Ngok Li, M. Di Renzo, and L.Hanzo, "A vision and an evolutionary framework for 6G: Scenarios, capabilities and enablers," 2023, *arXiv:2305.13887*.

[2] F. Shu et al., "Low-complexity and high-resolution DOA estimation for hybrid analog and digital massive MIMO receive array," *IEEE Trans. Commun.*, vol. 66, no. 6, pp. 2487–2501, Jun. 2018.

[3] M. D. Renzo et al., "Smart radio environments empowered by reconfigurable intelligent surfaces: How it works, state of research,and the road ahead," *IEEE J. Sel. Areas Commun.*, vol. 38, no. 11, pp. 2450–2525, Nov. 2020.

[4] H. He, S. Jin, C.-K. Wen, F. Gao, G. Y. Li, and Z. Xu, "Model-driven deep learning for physical layer communications," *IEEE Wireless Commun.*, vol. 26, no. 5, pp. 77–83, Oct. 2019.

[5] Q. Wu and R. Zhang, "Intelligent reflecting surface enhanced wireless network via joint active and passive beamforming," *IEEE Trans. Wireless Commun.*, vol. 18, no. 11, pp. 5394–5409, Nov. 2019.

[6] H. He, C.-K. Wen, S. Jin, and G. Y. Li, "Model-driven deep learning for MIMO detection," *IEEE Trans. Signal Process.*, vol. 68, pp. 1702–1715, Mar. 2020.

[7] R. Alghamdi et al., "Intelligent surfaces for 6G wireless networks: A survey of optimization and performance analysis techniques," *IEEE Access*, vol. 8, pp. 202795–202818, 2020.

[8] L. Dong and H.-M. Wang, "Enhancing secure MIMO transmission via intelligent reflecting surface," *IEEE Trans. Wireless Commun.*, vol. 19, no. 11, pp. 7543–7556, Nov. 2020.

[9] M. Di Renzo et al., "Reconfigurable intelligent surfaces vs. relaying: Differences, similarities, and performance comparison," *IEEE Open J. Commun. Soc.*, vol. 1, pp. 798–807, 2020.

[10] E. Basar, M. Di Renzo, J. De Rosny, M. Debbah, M.-S. Alouini, and R. Zhang, "Wireless communications through reconfigurable intelligent surfaces," *IEEE Access*, vol. 7, pp. 116753–116773, 2019.

[11] Q. Wu and R. Zhang, "Towards smart and reconfigurable environment: Intelligent reflecting surface aided wireless network," *IEEE Commun. Mag.*, vol. 58, no. 1, pp. 106–112, Jan. 2020.

[12] L. Dai et al., "Reconfigurable intelligent surface-based wireless communications: Antenna design, prototyping, and experimental results," *IEEE Access*, vol. 8, pp. 45913–45923, 2020.

[13] P. Wang, J. Fang, X. Yuan, Z. Chen, and H. Li, "Intelligent reflecting surface-assisted millimeter wave communications: Joint active and passive precoding design," *IEEE Trans. Veh. Technol.*, vol. 69, no. 12, pp. 14960–14973, Dec. 2020.

[14] C. Huang, A. Zappone, G. C. Alexandropoulos, M. Debbah, and C. Yuen, "Reconfigurable intelligent surfaces for energy efficiency in wireless communication," *IEEE Trans. Wireless Commun.*, vol. 18, no. 8, pp. 4157–4170, Aug. 2019.

[15] Z. Chu, W. Hao, P. Xiao, and J. Shi, "Intelligent reflecting surface aided multi-antenna secure transmission," *IEEE Wireless Commun. Lett.*, vol. 9, no. 1, pp. 108–112, Jan. 2020.

[16] Q. Li, M. El-Hajjar, I. Hemadeh, A. Shojaeifard, A. A. M. Mourad, and L. Hanzo, "Reconfigurable intelligent surface aided amplitude and phase-modulated downlink transmission," *IEEE Trans. Veh. Technol.*, vol. 72, no. 6, pp. 8146–8151, Jun. 2023.

[17] Q. Zheng, M. Wen, Q. Li, G. C. Alexandropoulos, and L. Xu, "Progressive channel estimation for single-carrier communications aided by reconfigurable intelligent surfaces," *IEEE Wireless Commun. Lett.*, vol. 12, no. 12, pp. 1993–1997, Dec. 2023.

[18] Z. Zhang et al., "Active RIS vs. passive RIS: Which will prevail in 6G?" *IEEE Trans. Commun.*, vol. 71, no. 3, pp. 1707–1725, Mar. 2023.

[19] K. Zhi, C. Pan, H. Ren, K. K. Chai, and M. Elkashlan, "Active RIS versus passive RIS: Which is superior with the same power budget?" *IEEE Commun. Lett.*, vol. 26, no. 5, pp. 1150–1154, May 2022.

[20] W. Lv, J. Bai, Q. Yan, and H. M. Wang, "RIS-assisted green secure communications: Active RIS or passive RIS?" *IEEE Wireless Commun. Lett.*, vol. 12, no. 2, pp. 237–241, Feb. 2023.

[21] Y. Li, C. You, and Y. J. Chun, "Active-IRS aided wireless network: System modeling and performance analysis," *IEEE Commun. Lett.*, vol. 27, no. 2, pp. 487–491, Feb. 2023.

[22] X. Li, C. You, Z. Kang, Y. Zhang, and B. Zheng, "Double-Active-IRS aided wireless communication with total amplification power constraint," *IEEE Commun. Lett.*, vol. 27, no. 10, pp. 2817–2821, Oct. 2023.

[23] X. Yang, H. Wang, and Y. Feng, "Sum rate maximization for active RIS-aided uplink multi-antenna NOMA systems," *IEEE Wireless Commun. Lett.*, vol. 12, no. 7, pp. 1149–1153, Jul. 2023.

[24] F. Shu et al., "Three high-rate beamforming methods for active IRS-aided wireless network," *IEEE Trans. Veh. Technol.*, vol. 72, no. 11, pp. 15052–15056, Nov. 2023.

[25] Q. Li, M. El-Hajjar, I. Hemadeh, D. Jagyasi, A. Shojaeifard, and L. Hanzo, "Performance analysis of active RIS-aided systems in the face of imperfect CSI and phase shift noise," *IEEE Trans. Veh. Technol.*, vol. 72, no. 6, pp. 8140–8145, Jun. 2023.

[26] Y. Wang et al., "Asymptotic performance analysis of large-scale active IRS-aided wireless network," *IEEE Open J. Commun. Soc.*, vol. 4, pp. 2684–2696, 2023.

[27] J. Yuan, G. Chen, M. Wen, D. Wan, and K. Cumanan, "Security-reliability tradeoff in UAV-carried active RIS-assisted cooperative networks," *IEEE Commun. Lett.*, vol. 28, no. 2, pp. 437–441, Feb. 2024.

[28] B. Qiu, W. Cheng, and W. Zhang, "Decomposed and distributed directional modulation for secure wireless communication," *IEEE Trans. Wireless Commun.*, vol. 23, no. 5, pp. 5219–5231, May 2024.

[29] F. Shu et al., "Directional modulation: A physical-layer security solution to B5G and future wireless networks," *IEEE Netw.*, vol. 34, no. 2, pp. 210–216, Mar./Apr. 2020.

[30] Y. Teng et al., "Low-complexity and high-performance receive beamforming for secure directional modulation networks against an eavesdropping-enabled full-duplex attacker," *Sci. China Inf. Sci.*, vol. 65, no. 1, pp. 119302–119302, Jan. 2022.

[31] F. Shu, X. Wu, J. Hu, J. Li, R. Chen, and J. Wang, "Secure and precise wireless transmission for random-subcarrier-selection-based directional modulation transmit antenna array," *IEEE J. Sel. Areas Commun.*, vol. 36, no. 4, pp. 890–904, Apr. 2018.

[32] F. Shu et al., "Enhanced secrecy rate maximization for directional modulation networks via IRS," *IEEE Trans. Commun.*, vol. 69, no. 12, pp. 8388–8401, Dec. 2021.

[33] R. Dong, S. Jiang, X. Hua, Y. Teng, F. Shu, and J. Wang, "Low-complexity joint phase adjustment and receive beamforming for directional modulation networks via IRS," *IEEE Open J. Commun. Soc.*, vol. 3, pp. 1234–1243, 2022.

[34] Y. Lin, B. Shi, F. Shu, R. Dong, P. Zhang, and J. Wang, "Enhanced secure wireless transmission using IRS-aided directional modulation," *IEEE Trans. Veh. Technol.*, vol. 72, no. 12, pp. 16794–16798, Dec. 2023.

[35] C. Pan et al., "Multicell MIMO communications relying on intelligent reflecting surfaces," *IEEE Trans. Wireless Commun.*, vol. 19, no. 8, pp. 5218–5233, Aug. 2020.

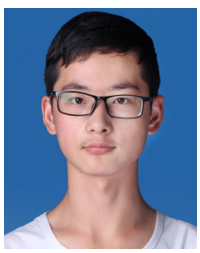

KE YANG received the B.E. degree from Nanchang University, China, in 2021. He is currently pursuing the M.S. degree with the School of Information and Communication Engineer, Hainan University, China. His research interests include physical layer security and intelligent reflecting surface.

RONGEN DONG is currently pursuing the Ph.D. degree with the School of Information and Communication Engineer, Hainan University, China. Her research interests include physical layer security and directional modulation networks.

WEI GAO received the B.E. degree in communication engineering and the Ph.D. degree of information and communication engineering from the Huazhong University of Science and Technology in 2014 and 2020, respectively. He is currently a Postdoctoral Fellow with Hainan University. His research interests include network architecture, wireless network access, and radio resources allocation.

FENG SHU (Member, IEEE) was born in 1973. He received the B.S. degree from Fuyang Teaching College, Fuyang, China, in 1994, the M.S. degree from Xidian University, Xi'an, China, in 1997, and the Ph.D. degree from Southeast University, Nanjing, China, in 2002. From 2009 to 2010, he was a Visiting Postdoctoral Fellow with the University of Texas at Dallas, Richardson, TX, USA. From July 2007 to September 2007, he was a Visiting Scholar with the Royal Melbourne Institute of Technology, Melbourne, VIC, Australia. From 2005 to 2020, he was with the School of Electronic and Optical Engineering, Nanjing University of Science and Technology, Nanjing, where he was promoted from an Associate Professor to a Full Professor of supervising Ph.D. students in 2013. Since 2020, he has been with the School of Information and Communication Engineering, Hainan University, Haikou, China, where he is currently a Professor and a Supervisor of Ph.D. and graduate students. He has authored or coauthored more than 300 in archival journals with more than 150 papers on IEEE journals and 250 SCI-indexed papers. His citations are more than 8000 times. He holds one U.S. patent and more than 40 Chinese patents. He is also a PI or a Co-PI for eight national projects. His research interests include wireless networks, wireless location, and array signal processing. He was awarded with the Leading-Talent Plan of Hainan Province in 2020, the Fujian Hundred-Talent Plan of Fujian Province in 2018, and the Mingjian Scholar Chair Professor in 2015. He was an Exemplary Reviewer for IEEE TRANSACTIONS ON COMMUNICATIONS in 2020. He is currently an Editor of IEEE WIRELESS COMMUNICATIONS LETTERS and a Guest Editor for the *Chinese Journal of Aeronautics* and *Journal of Electronics and Information Technology* He was an Editor of IEEE SYSTEMS JOURNAL from 2019 to 2021 and IEEE ACCESS from 2016 to 2018, and also a Guest Editor of *IET Communications* and *Security and Safety*.

WEIPING SHI received the M.S. degree from the Chongqing University of Posts and Telecommunications, China, in 2014, and the Ph.D. degree from the School of Electronic and Optical Engineering, Nanjing University of Science and Technology, China, in 2023. She is currently a Teacher with the School of Network and Communication, Nanjing Vocational College of Information Technology, Nanjing, China. Her research interests include IRS-aided wireless communication and physical layer security.

YAN WANG is currently pursuing the Ph.D. degree with the School of Information and Communication Engineer, Hainan University, China. Her research interests include the performance analysis of wireless communication systems, spatial modulation, and intelligent reflecting surface.

XUEHUI WANG received the M.S. degree from Hainan University, China, in 2020, where she is currently pursuing the Ph.D. degree with the School of Information and Communication Engineering. Her research interests include wireless communication, signal processing, and IRS-aided relay systems.

JIANGZHOU WANG (Fellow, IEEE) is a Professor with the University of Kent, U.K. He has published more than 500 papers and five books. His research focuses on mobile communications. He was a recipient of the 2022 IEEE Communications Society Leonard G. Abraham Prize. He was the Technical Program Chair of the 2019 IEEE International Conference on Communications, Shanghai, the Executive Chair of the IEEE ICC2015, London, and the Technical Program Chair of the IEEE WCNC 2013. He is/was an Editor of a number of international journals, including IEEE TRANSACTIONS ON COMMUNICATIONS from 1998 to 2013. He is a Foreign Member of the Chinese Academy of Engineering, and a Fellow of the Royal Academy of Engineering, U.K., and of IET.